AD-A253 562

Final Report for:

Office of Naval Research

Contract Number N00014-89-K-0149

funded by:

Strategic Defense Initiative IST Program

for Period between

May 15, 1989 through December 31, 1990

Project Title: "Advanced Transport Systems for Electron Beams in High Brightness Accelerators and FELs",

Principal Investigator: Ronald M. Gilgenbach

Co-PIs: T. Kammash and M. L. Brake

Intense Energy Beam Interaction Lab

Nuclear Engineering Department

University of Michigan

Ann Arbor, MI 48109-2104

March 1991

REPORT DOCUMENTATION PAGE

Form Approved
OMB No. 0704-0188

1. AGENCY USE ONLY *(Leave blank)*

2. REPORT DATE
3/20/91

3. REPORT TYPE AND DATES COVERED
Final:5-15-89 to 12-31-90

4. TITLE AND SUBTITLE
Advanced Transport Systems for Electron Beams in High Brightness Accelerators and FELs

5. FUNDING NUMBERS
ONR Contract
SFRC Number
N00014-89-K-0149

6. AUTHOR(S)
R. M. Gilgenbach, T. Kammash

7. PERFORMING ORGANIZATION NAME(S) AND ADDRESS(ES)
Nuclear Engineering Department
University of Michigan
Ann Arbor, MI 48109-2104

8. PERFORMING ORGANIZATION REPORT NUMBER

9. SPONSORING/MONITORING AGENCY NAME(S) AND ADDRESS(ES)
Strategic Defense Initiative
Innovative Science and Technology/
Office of Naval Research

10. SPONSORING/MONITORING AGENCY REPORT NUMBER

11. SUPPLEMENTARY NOTES

12a. DISTRIBUTION/AVAILABILITY STATEMENT

Approved for public release;
distribution is unlimited.

12b. DISTRIBUTION CODE

13. ABSTRACT *(Maximum 200 words)*

Experiments have been performed to investigate the beam-breakup-instability in electron beam transport through cavity systems. A ten cavity system with solenoidal magnetic transport has been developed. Two accelerators at the University of Michigan are applicable to these experiments:
1) Febetron with long-pulse modules operating at parameters: voltage=0.4 MV, diode current = 1 kA, extracted current = 20-100 A, and pulselength = 0.3 μs. The MELBA accelerator operates at parameters: voltage =-0.8 to -1MV, diode current = 1-30 kA, extracted current= 0.1 to 0.4 kA, and pulselength= 1-2 μs. Initial experiments performed on a 10 cavity system on the Febetron showed 42 dB of RF growth at the TM_{110} resonance frequency of 2.5 GHz. The experimental growth length is within a factor of two of that predicted by theory. Experiments in the strong focusing regime showed a strong dependence on magnetic field, as expected. Theoretical research has solved the x-y coupled differential equations of the BBU instability and shown that in the strong-focusing regime, the x-y coupling yields two wave modes identical to the 1-D case, except at twice the coupling constant. Theoretical research has also shown that ion channels reduce the BBU growth rate.

14. SUBJECT TERMS
Electron beams, accelerators

15. NUMBER OF PAGES
23

16. PRICE CODE

17. SECURITY CLASSIFICATION OF REPORT	18. SECURITY CLASSIFICATION OF THIS PAGE	19. SECURITY CLASSIFICATION OF ABSTRACT	20. LIMITATION OF ABSTRACT
UNCLASSIFIED	UNCLASSIFIED	UNCLASSIFIED	

NSN 7540-01-280-5500

Standard Form 298 (Rev 2-89)
Prescribed by ANSI Std 239-18

Table of Contents

1.0 Technical Description of Progress

1.1 Experimental Progress

During the period of this contract an experiment was designed, built and tested for investigations of the transport and stability of long pulse electron beams through cavity systems. Figure 1 depicts the experimental configuration for this research. A ten cavity system was fabricated and cold-tested with a TM_{110} resonance frequency at 2.5 GHz. This frequency was chosen for two reason: first, it corresponds to the S-band, where we have an extensive array of experimental equipment, including a high power pulsed microwave source. Second, the length of the cavities was chosen as 1/4 RF cycle for an electron transit time, yielding a convenient cavity length of about 2 cm. Each cavity was fabricated with a microwave coupling loop oriented to detect the TM_{110} cavity mode which is subject to the beam breakup instability. Cold-tests were performed on each of the ten cavities with the *results summarized in Table 1. It can be seen that* the cavity resonance frequency (2.51 GHz $\pm$ 0.002) and Q are very well controlled (Q= 210 $\pm$ 30). Cavities were isolated by short cutoff sections of copper tube. The cavities were placed inside a 6 inch diameter tube which acted as both a vacuum chamber and solenoid. The capacitor bank driving this solenoid was upgraded to a two-stage, SCR switched, Marx generator, with double sided charging of ($\pm$ 450 V) electrolytic capacitor banks. This permitted a solenoidal magnetic field of up to 5 kG.

Initial experiments were performed on a moderate size electron beam generator (Febetron) with long-pulse modules, operating at parameters given in Table 2. Initial experiments compared velvet versus carbon brush cathodes. The carbon brush cathode was chosen for its ability to generate a uniform pencil beam. A graphite anode was employed

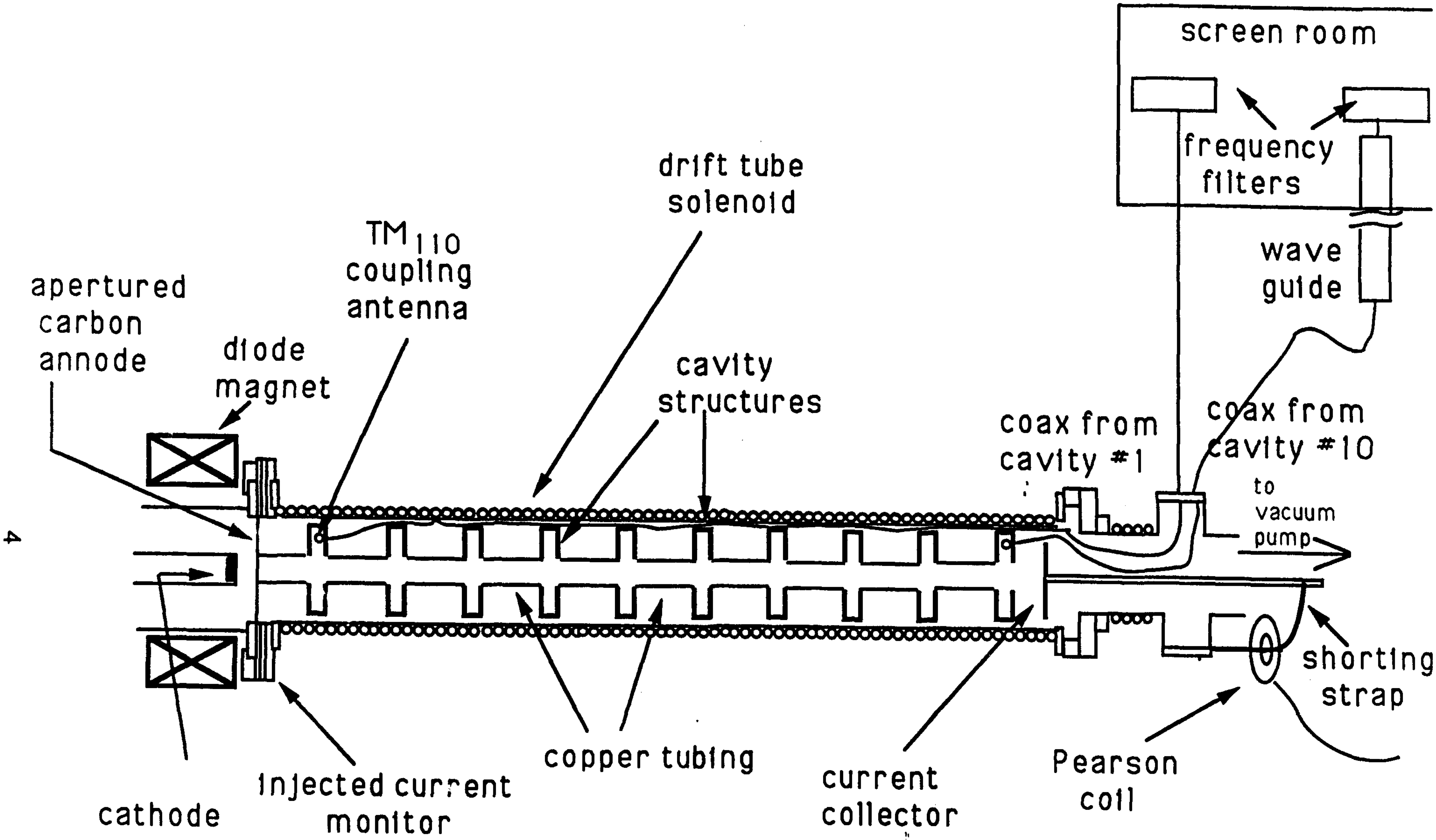

Figure 1. Experimental Configuration.

with a circular aperture which gave extracted currents of 20 to 100 A, well below the vacuum-limiting current in the six inch solenoid tube.

Signals from the RF coupling loops in the first (or second) cavity and the last cavity were run from semi-rigid coaxial cable to the Faraday cage for measurement of frequency and power. By adding attenuation to the signal frcm the later cavities we can measure the RF gain as the e-beam is transported through the cavities. Electron beam current is measured at the injection point by a Rogowski coil in the flange and after transport through the cavities by a collector connected to ground though a Pearson current transformer.

Data from electron beam transport in a ten cavity system is given in the attached paper from the SPIE conference. The data show that the RF signal at the 2.5 GHz frequency is amplified by 42 dB in propagating through a ten cavity system. Further details are given in the SPIE paper, however, it should be noted that the e-folding length and the growth-time for the RF are in reasonable agreement (factor of two) with the theoretical predictions. Differences may arise because the continuum theory may not be valid for this small number of cavities. The Febetron data gave slightly different results than an initial set of experiments performed on MELBA with a five cavity experiment. The Febetron data showed a strong dependence on magnetic field, compared to the MELBA data which was almost independent of B. This behavior is expected since the Febetron is in the strong focusing regime and MELBA operates in the weak focusing regime.

TABLE 1

Microwave Cavity Parameters for

Beam Breakup Instability Experiments

Cavity Radius	6.9 cm
Cavity TM110 Mode Frequency	2.51 ± 0.002 GHz
Cavity Q	210 ± 30
Number of Cavities	10
Vaccum Chamber Inside Diameter	7.4 cm

TABLE 2. Parameters of Accelerators at University of Michigan

Parameter	***Febetron***	***MELBA***
Beam Voltage:	-0.3 MV	-0.7 to -1.0 MV
Diode Beam Current:	1 kA	1 - 30 kA
Extracted Beam Current	0.02-0.1 kA	0.1-0.4 kA
Electron beam Pulselength:	0.3 μs	1 to 4 μs

1.2 Theoretical Progress

Theoretical research has addressed several issues. One issue concerns the effect of X-Y coupling on the growth rate for the beam-breakup-instability in a solenoidal magnetic field. We have solved the x-y coupled differential equations and compared the resulting dispersion relation to the 1-D result of Y.Y. Lau. Our results show that in the strong-focusing regime, the x-y coupling yields two wave modes, which are identical to the 1-D description, except at twice the coupling constant. As expected, our 2-D result in the weak focusing regime is the same as the 1-D description. This research was recently published in Applied Physics Letters.

Another important analytical problem associated with the BBU instability is the effect of an e-beam-induced ion channel at low pressures. We have examined the cumulative BBU utilizing a rigid beam model, and derived a dispersion equation that we analyzed in various parameter regimes. Assuming that e-beam impact ionization is the only ionization mechanism, we found that the ion channel by itself could not stabilize the BBU instability, but it could reduce the growth rate substantially ($\sim 10^{-2}$). Upon introducing the beam betatron frequency spread we observed that this leads to narrowing the unstable mode range, but does not change the results in any major fashion.

2.0 Personnel Supported by Contract

Faculty Supported by This Contract

1) R. M. Gilgenbach, Professor
2) T. Kammash, Professor
3) M.L. Brake, Associate Professor

Graduate Students Receiving Support from this Contract

1) T. Repetti
2) Peter Menge
3) J.J. Choi

Postdoctoral Researchers Supported by This Contract

1) R. A. Bosch

3.0 Doctoral Dissertations Concerning this Project

1) Peter Menge, " Investigations of the Beam Breakup Instability in Electron Beam Transport Through Cavity Systems", (research in Progress)

4.0 Publications Concerning This Project

1) "Effects of X-Y Coupling on the Beam Breakup Instability", R.A. Bosch and R. M. Gilgenbach, Applied Physics Letters, **58** 699 (1991)

2) "Experiments on The BBU Instability in Long-Pulse Electron Beam Transport Through Cavity Systems", P.R. Menge, R.A. Bosch, R.M. Gilgenbach, J.J. Choi, H. Ching, and T.A. Spencer, Proceeding of the SPIE's OE LASE'91, SPIE Proceedings Number 1407, 1991

5.0 Conference Presentations Concerning This Project

1) Thirty Fifth Annual Meeting of the Division of Plasma Physics of the American Physical Society, Nov. 12-16, 1990, Cincinnati, Ohio

2) "Experiments on The BBU Instability in Long-Pulse Electron Beam Transport Through Cavity Systems", P.R. Menge, R.A. Bosch, R.M. Gilgenbach, J.J. Choi, H. Ching, and T.A. Spencer, Presented at the SPIE's OE LASE'91, January 1991, Los Angeles, CA.

Effect of x-y coupling on the beam breakup instability

R. A. Bosch and R. M. Gilgenbach
Intense Energy Beam Interaction Laboratory, Nuclear Engineering Department, The University of Michigan, Ann Arbor, Michigan 48109-2104

(Received 4 September 1990; accepted for publication 13 November 1990)

In solenoidal beam transport systems, motions in the x and y directions are coupled by the $\mathbf{v}\times\mathbf{B}$ force. A two-dimensional coupled mode description of the beam breakup (BBU) instability is presented; its dispersion relation is derived and compared with the one-dimensional BBU dispersion relation. In the two-dimensional description, instability growth is doubled and two additional wave modes are found in the regime of strong focusing. In the weak focusing regime, the two-dimensional description gives the same dispersion relation as the one-dimensional model.

We examine the effect of coupling between the x and y directions of transverse motion in the beam breakup (BBU) instability. A dispersion relation is derived from a two-dimensional coupled-mode description, yielding four wavemodes. In the strong focusing regime, two of these modes are identical to those found with the existing one-dimensional theory, but with twice the coupling constant. In addition, we find two modes not given by the one-dimensional theory. In the weak focusing regime, our results reduce to the dispersion relation found by one-dimensional theory. This is expected because x-y coupling vanishes in the weak focusing limit.

Existing descriptions of the BBU instability have considered the interaction of an electron (or ion) beam with linearly polarized microwave oscillations in cylindrical pillbox cavities. Calculations in different regimes[1-3] have recently been unified by a one-dimensional coupled-mode theory[4] which reproduces the earlier findings in their regimes of validity. This coupled-mode theory also shows a different scaling in a previously undescribed regime.

The one-dimensional coupled-mode equations are[4]

$$\frac{d}{dt}\gamma\frac{dx}{dt}+\gamma\omega_c^2x=a, \tag{1a}$$

$$\left(\frac{\partial^2}{\partial t^2}+\frac{\omega_0}{Q}\frac{\partial}{\partial t}+\omega_0^2\right)a=2\gamma\omega_0^4\epsilon x, \tag{1b}$$

where $\gamma=(1-\beta^2)^{-1/2}$ is the relativistic mass factor, ω_c is the betatron frequency ($\omega_c=eB/mc\gamma$ is the relativistic electron cyclotron frequency in a solenoidal field), and $d/dt=\partial/\partial t+v\partial/\partial z$ is the convective derivative.

Assuming a disturbance of the form $e^{i\omega t-ikz}$, these equations yield the dispersion relation

$$\Omega^2-(\omega_c^2-\Gamma)=0, \tag{2}$$

where $\Omega=\omega-kv$ and $\Gamma=2\omega_0^4\epsilon/(-\omega^2+\omega_0^2+i\omega\omega_0/Q)$.

In a solenoidal magnetic field, the magnetic force is a velocity-dependent force coupling the x and y motions, so that a one-dimensional description, such as given by Eq. (1), may be inadequate.[5] In particular, the description of the focusing force as a harmonic potential force ($\gamma\omega_c^2x$) may be inaccurate for solenoidal focusing. In order to examine this possibility for the BBU instability, we use a coupled-mode description which describes motion in both the x and y directions, which are transverse to the beam.

We consider a magnetized beam ($\omega_{pe}<\omega_{ce}$) in a solenoid, passing through cylindrical cavities whose radius is large compared to the beam radius, and whose length and spacing are small compared to the scale length of the beam disturbance. The TM_{110} frequency of the cavities is denoted ω_0. The cyclotron motion of the magnetized beam couples the transverse motions in the x and y directions. The equation of motion for a beam influenced by the transverse force per unit mass $\mathbf{a}(z,t)$ is

$$\frac{d}{dt}\gamma\frac{dx}{dt}+\gamma\omega_c\frac{dy}{dt}=a_x, \tag{3a}$$

$$\frac{d}{dt}\gamma\frac{dy}{dt}-\gamma\omega_c\frac{dx}{dt}=a_y, \tag{3b}$$

where $\gamma=(1-\beta^2)^{-1/2}$ is the relativistic mass factor, $\omega_c=eB/mc\gamma$ is the relativistic electron cyclotron frequency in the solenoidal field, and $d/dt=\partial/\partial t+v\partial/\partial z$ is the convective derivative.

The TM_{110} modes are excited by e-beam displacements according to

$$\left(\frac{\partial^2}{\partial t^2}+\frac{\omega_0}{Q}\frac{\partial}{\partial t}+\omega_0^2\right)a_x=2\gamma\omega_0^4\epsilon x, \tag{4a}$$

$$\left(\frac{\partial^2}{\partial t^2}+\frac{\omega_0}{Q}\frac{\partial}{\partial t}+\omega_0^2\right)a_y=2\gamma\omega_0^4\epsilon y, \tag{4b}$$

where Q is the quality factor of the microwave cavity. The mode giving rise to force a_x is the linearly polarized mode with magnetic field in the y direction on axis, while a_y arises from the orthogonal linearly polarized mode. Equations (3) and (4) are invariant under rotation in the x-y plane. The quantity ϵ is the dimensionless coupling constant of the e-beam to the TM_{110} mode, given by[6]

$$\epsilon=0.422(l/L)(I/17kA)\beta/\gamma, \tag{5}$$

where l is the length of the microwave cavities, L is their spacing, and I is the beam current. For disturbances with

10

$\omega_0 < 0$, Q must be replaced by $-Q$. This yields the same equations, henceforth we shall only consider $\omega_0 > 0$.

If we set $a_y = 0$ in Eq. (3b) and disregard Eq. (4b), we obtain the one-dimensional BBU description of Eq. (1), as well as the solution $x = c'y/dt = 0$, i.e., $\Omega = 0$. This situation would arise, e.g., if the microwave mode giving rise to a_y were negligible as a result of preferential damping, etc. In cases with cylindrical symmetry, both microwave modes may be excited, and their combination may not yield a linearly polarized wave. The two-dimensional description of transverse beam dynamics may be utilized in this case.

For a disturbance of form $e^{-i(kz-\omega t)}$, Eqs. (3) and (4) yield the dispersion relation

$$\Omega^4 + \Omega^2(-\omega_c^2 + 2\Gamma) + \Gamma^2 = 0, \tag{6}$$

where $\Omega = \omega - vk$, $\Gamma = 2\omega_0^4\epsilon/(-\omega^2 + \omega_0^2 + i\omega\omega_0/Q)$, and $\Gamma|_{\omega_0} = -2i\omega_0^2\epsilon Q$.

The resonant modes ($\omega = \omega_0$) obey

$$k|_{\omega_0} = \frac{1}{v}\left[\omega_0 \pm \left(\frac{\omega_c^2 + 4i\omega_0^2\epsilon Q \pm (\omega_c^4 + 8i\omega_0^2\omega_c^2\epsilon Q)^{1/2}}{2}\right)^{1/2}\right], \tag{7}$$

$$v\frac{\partial k}{\partial \omega}\bigg|_{\omega_0} = 1 \pm \left(\frac{\omega_c^2 + 4i\omega_0^2\epsilon Q \pm (\omega_c^4 + 8i\omega_0^2\omega_c^2\epsilon Q)^{1/2}}{2}\right)^{-1/2} \times [1 \pm \omega_c^2(\omega_c^4 + 8i\omega_0^2\omega_c^2\epsilon Q)^{-1/2}](\epsilon Q^2\omega_0) \times (2 - i/Q). \tag{8}$$

Equations (7) and (8) describe four resonant modes. Two of the modes have $\mathrm{Im}(k) > 0$, and thus can give rise to convective growth. Equation (8) is useful in estimating the group velocity of a disturbance with frequencies centered at ω_0 according to

$$v_g = [\mathrm{Re}(\partial k/\partial \omega)|_{\omega_0}]^{-1}. \tag{9}$$

The expected behavior of a disturbance (for sufficiently large time) is that it will be dominated by the fastest growing mode; i.e., $\omega = \omega_0$. The peak of the disturbance will move at the velocity given by Eq. (9), while its amplitude will evolve as $\mathrm{Im}(k)z$. In order to examine the amplitude at fixed z, the Green's function may be constructed from the dispersion relation.

In the limit of strong focusing ($|\Gamma|_{\omega_0}| \ll \omega_c^2$), the dispersion relation is approximated by

$$[\Omega^2 - (\omega_c^2 - 2\Gamma)][\Omega^2 - \Gamma^2/\omega_c^2] = 0. \tag{10}$$

For comparison, the dispersion relation of the one-dimensional description of the BBU[4] is $\Omega^2 - (\omega_c^2 - \Gamma) = 0$. For strong focusing, the modes obey

$$k|_{\omega_0} = (1/v)[\omega_0 \pm (\omega_c + 2i\omega_0^2\epsilon Q/\omega_c)], \tag{11a}$$

$$k|_{\omega_0} = (1/v)[\omega_0 \pm 2i\omega_0^2\epsilon Q/\omega_c], \tag{11b}$$

$$\mathrm{Re}(\partial k/\partial \omega|_{\omega_0}) = (1/v)(1 \pm 4\epsilon Q^2\omega_0/\omega_c). \tag{12}$$

Equation (12) describes the modes of (11a) and (11b). We note that the e-folding length of the growing modes [$\mathrm{Im}(k) > 0$] is the same for (11a) and (11b); the group velocities are also equal. The e-folding length is proportional to the magnetic field strength.

A growing disturbance described by Eq. (11a) [with the plus sign, so $\mathrm{Im}(k) > 0$] will propagate at the group velocity found with Eq. (12), growing as $\exp[\mathrm{Im}(k)z]$, where $\mathrm{Im}(k)$ is given by (11a). The growth rate is twice that found with the one-dimensional approach[2,7] [Eqs. (5.14) and (5.15) of Ref. 2], while the group velocity is reduced. This is a result of the factor of two multiplying Γ in the first factor of Eq. (10) which does not appear in Eq. (2).

In order to describe the modes of (11a) using the existent one-dimensional theory, it is sufficient to use double the value of coupling constant ϵ given by Eq. (5). This accounts for the existence of twice as many microwave modes as were included in the one-dimensional approach.

Two additional wave modes [Eq. (11b)], not found in the one-dimensional description, result from consideration of the coupling between x and y degrees of freedom. In the limit of low beam current ($\epsilon \to 0$), these modes have $\Omega = 0$, while the modes of Eq. (11a) have $\Omega = \pm(-\omega_c)$. The modes of Eq. (11b) have growth rates equal to those of Eq. (11a). Their contribution to the Green's function $\{G(z,t) \sim \int d\omega \exp[i\omega t - ik(\omega)z]\}$ has the same asymptotic response [multiplied by $\exp(i\omega_c z/v)$]. As a result, they may be expected to play a significant role in BBU growth.

In the case where the wavelengths of the convectively unstable modes [Eqs. (11a) and (11b) with plus signs] do not greatly exceed the lengths of the microwave cavities, finite transit time effects will reduce BBU growth.[8] The convectively unstable mode of Eq. (11b) has a longer wavelength, so that its growth reduction may be less severe. Thus, it may be the dominant unstable mode.

In the limit of weak focusing ($|\Gamma|_{\omega_0}| \gg \omega_c^2$), the dispersion relation reduces to

$$\Omega^4 + 2\Gamma\Omega^2 + \Gamma^2 = (\Omega^2 + \Gamma)^2 = 0, \tag{13}$$

$$k|_{\omega_0} = (1/v)\{\omega_0 \pm (1+i)\omega_0\epsilon^{1/2}Q^{1/2}\}, \tag{14}$$

$$\partial k/\partial \omega|_{\omega_0} = (1/v)[1 \pm (1-i)\epsilon^{1/2}Q^{3/2}(1 - i/2Q)]. \tag{15}$$

These solutions are identical to those obtained in the one-dimensional approach with weak focusing. For weak focusing, motion in the two transverse directions is decoupled, so that the one-dimensional and two-dimensional results are expected to be the same.

Using Eqs. (11), (12), (14), and (15), the BBU instability behavior can be modeled for strong or weak focusing. The wavelength of a resonant unstable mode is $\lambda = 2\pi/\mathrm{Re}(k)$, the e-folding length is $l_e = [\mathrm{Im}(k)]^{-1}$, the convective growth time is $\tau_e = l_e/v_g$. For a disturbance resulting from an impulse at $(z,t) = (0,0)$, the disturbance at position "z" will be maximum at the time $t_m = z/v_g$.

In summary, the effects of x-y coupling on the BBU instability have been examined with a two-dimensional description of the BBU instability. In the strong focusing regime, the x and y directions of motion are coupled, so that the two-dimensional description yields results not

11

found in the one-dimensional description with harmonic focusing force. Two wave modes are found which are identical to those of the one-dimensional description for twice the coupling constant. Two additional modes are found which do not appear in the one-dimensional approach.

In the weak focusing regime, the two-dimensional description gives the same dispersion relation as the one-dimensional model.

We acknowledge valuable discussions with Y. Y. Lau. This research was supported by SDIO through an Office of Naval Research contract.

[1] W. K. H. Panofsky and M. Bander, Rev. Sci. Instrum. 39, 206 (1968).
[2] V. K. Neil, L. S. Hall, and R. K. Cooper, Part. Accel. 9, 213 (1979).
[3] A. W. Chao, B. Richter, and C. Y. Yao, Nucl. Instrum. Methods 178, 1 (1980).
[4] Y. Y. Lau, Phys. Rev. Lett. 63, 1141 (1989); Y. Y. Lau, Phys. Rev. Lett. 63, 2433 (1989).
[5] D. Chernin, Part. Accel. 24, 29 (1988).
[6] Y. Y. Lau, NRL Memo Report No. 6237, 1988.
[7] G. J. Caporaso, A. G. Cole, and K. W. Struve, IEEE Trans. Nucl. Sci. NS-30, 2507 (1983).
[8] Y. Y. Lau (private communication).

Presented at the SPIE's OE/LASE '91
January 20-25, 1991, Los Angeles, California

EXPERIMENTS ON THE BBU INSTABILITY IN LONG-PULSE ELECTRON BEAM TRANSPORT THROUGH CAVITY SYSTEMS

P.R. Menge, R.A. Bosch, R.M. Gilgenbach, J.J. Choi, H. Ching, and T.A. Spencer

Intense Energy Beam Interaction Laboratory, Department of Nuclear Engineering
Cooley Building, North Campus, The University of Michigan, Ann Arbor, Michigan
48109-2104

ABSTRACT

Experiments have been performed to investigate the beam breakup (BBU) instability in electron beams transported through RF cavity systems. Experiments have utilized two accelerators: 1) a Febetron accelerator operating with energy = 100-300 keV, extracted current = 10-100 A, and pulse length = 300 ns and 2) the Michigan Electron Long Beam Accelerator (MELBA), with energy = 0.6-0.9 MeV, extracted current = 100-400 A and pulselength = 0.5-2 μs. The transport system consists of 5 or 10 RF cavities with Q = 210 ± 30. The cavities are connected by cutoff waveguide sections, which prevent electromagnetic coupling between cavities in order to eliminate the regenerative BBU. Each cavity has a microwave probe to detect growth of e-beam emission in the non-axisymmetric TM_{110} mode at 2.5 GHz, corresponding to the BBU. Solenoidal magnetic fields of 1-3.5 kG are applied. Initial experimental data on the Febetron show strong (>40 dB) growth of RF at 2.5 GHz between the first and tenth cavity. MELBA data shows about 20 dB RF growth between the 2nd and 5th cavities in a 5 cavity system. Up to 85% of the injected current is transported through the cavity system. The magnitude of BBU growth, its dependence on current and magnetic field, and the onset time to RF peaking are consistent with theory.

1. INTRODUCTION

The beam breakup instability (BBU) is a primary problem in the development of high-brightness, long-pulse linear electron accelerators. The BBU instability is caused by an unstable coupling between the transverse motion of the charged particle beam and a non-axisymmetic mode of the accelerating cavities,[1-4] e.g. the TM_{110} resonant cavity mode. BBU growth is a concern because it can cause a number of effects ranging from the loss of beam quality to the total loss of beam to the walls of the accelerator[1]. Experiments at the University of Michigan are directed toward acquiring a greater understanding of BBU with the particular purpose of discovering its associated scaling laws and uncovering techniques to suppress the BBU. The initial experiments on diagnosing and identifying the BBU are presented here.

2. EXPERIMENTAL CONFIGURATION

Two long-pulse electron beam accelerators were employed in this research: 1) a Febetron generator with diode parameters: voltage=100-300 kV, current=1 kA, and pulselength=300 ns, 2) Michigan Electron Long Beam Accelerator (MELBA) with diode

parameters: voltage=0.6-0.9 MV, current=10 kA, pulselength=0.5-2 μs. A comparison of the two accelerators is presented in Table 1.

Initial experiments were performed on the Febetron generator. The experimental configuration is depicted in Figure 1. The electron beam is generated from a planar brush cathode in a shielded area of the cathode stalk. The anode consists of a circular carbon plate with a 1.0 cm diameter aperture at the center, which allows 20 - 100 A to pass through, depending on the magnetic field. The diode and drift tube are immersed in a uniform magnetic field that can be varied from 1000 - 5000 G. This magnetic field is produced by a solenoid wound directly on the diode and drift tube regions; an SCR-switched $\pm$ 900 V double-sided electrolytic capacitor bank drives the solenoid. The experiments were performed in vacuum on the order of 10^{-5} Torr.

Inside the drift tube are ten brass resonant cavities with the dimensions of: inner radius of 6.9 cm and length of 2.0 cm. The cold-test RF parameters of these cavities are: TM_{110} mode frequency = 2.51 GHz $\pm$ 0.2%, Q = 210 $\pm$ 30 (see Table 2). The cavities are separated by smaller diameter copper tubes (ID = 3.4 cm, length = 3 cm or 1 cm) whose purpose is to cut off the propagation of the fundamental modes arising in the cavities, in effect electromagnetically isolating each cavity. Holes are drilled in these small diameter tubes to facilitate vacuum pumping.

Inside the end wall of each cavity is a small circular antenna designed for maximum coupling with the TM_{110} mode. The RF signal picked up by the antenna is transmitted through a semi-rigid coaxial cable to the outside of the vacuum chamber. The signal is then transmitted via RG/8 coax to either an S-band waveguide to the Faraday cage or directly to the Faraday cage. Inside the Faraday cage, RF frequency and signal strength were measured using frequency filters and diode detectors, respectively. In these initial Febetron experiments only the RF from the first and the 10^{th} cavities was measured. Frequency filters were used at 2.5 GHz corresponding to the TM_{110} mode and 1.6 GHz corresponding to the TM_{010} mode.

The electron beam current is measured before entering the first cavity and after exiting the last cavity. The entering current is measured using a Rogowski coil imbedded in the anode flange. The exiting current is measured by means of a collector plate connected to ground with a conducting strap; a Pearson coil is placed around the strap to measure the return current flowing to ground. The injected currents used in these Febetron experiments were in the range of 20 - 100 A.

Preliminary experiments have also been performed on the Michigan Electron Long Beam Accelerator (MELBA). The MELBA electron beam is generated from a planar velvet cathode in a shielded guard ring. This cathode has been shown to exhibit low diode closure velocities, permitting multimicrosecond e-beam pulselengths. Large diameter magnetic field coils are used in the diode region; these are pulsed by an ignitron-switched capacitor bank. The diode magnetic field was kept at a constant 800 G for the experiments reported here. The anode is a circular carbon plate with a 2 cm diameter aperture which extracts 100-400 A. The rest of the MELBA experiment is identical to the Febetron configuration except that only 5 resonant cavities were used, and that RF was measured in the second and fifth cavities.

The advantage of using these two accelerators is that their differing parameters result in BBU growth in two different growth regimes. The electron beam produced by the Febetron falls into the growth regime of "strong focusing",[5,6] while MELBA produces a

beam in the "weak focusing"[1,5] region. This provides the opportunity to examine the scaling of the beam breakup instability.

3. EXPERIMENTAL RESULTS AND DISCUSSION

3.1 Febetron Experimental Results and Discussion

Measurements were made of the RF emission detected by probes in at least 2 cavities per experimental run. Data from two shots is shown in Figure 2, for the case where the microwave cavities were separated by copper tubes of 3 cm length (cavity spacing = 6 cm). The uppermost trace is the diode detector signal from the antenna in the 10^{th} cavity. The signal passed through a frequency filter centered at 2.5 GHz (bandwidth = 20 MHz) after it had been attenuated by 45 dB. The next trace is the diode detector signal from the first cavity; it has not been filtered for frequency except by the S-band waveguide (>1.7 GHz). This signal has been attenuated by only 3 dB. The center trace is the Febetron voltage signal. The bottom two traces are the transported and injected currents respectively. The microwave power was found to increase by approximately 42 dB between the first and 10th cavities; the RF power in the 10th cavity was primarily at 2.5 GHz, the expected BBU frequency. When the experiment was repeated with microwave cavities separated by copper tubes of 1 cm (spacing = 3 cm), similar results were obtained, with microwave growth of 40 dB between the first and the 10th cavities.

Figure 3 shows the fraction of current transported as a function of the applied magnetic field. The fraction of current that was transported was found to increase nearly linearly with the magnetic field from zero at no applied magnetic field to 100 A at 4.5 kG (the highest field applied).

From the Febetron data, four comparisons with BBU theory were obtained. A two-dimensional mode-coupling model of BBU growth[7] predicts a dispersion relation for two convectively-growing BBU wavemodes in the strong focusing regime:

$$k(\omega_o) = (1/v)(\omega_o + \omega_c + 2i\omega_o^2\, \varepsilon\, Q/\omega_c), \text{ and}$$
$$k(\omega_o) = (1/v)(\omega_o + 2i\omega_o^2\, \varepsilon\, Q/\omega_c) \qquad (1)$$

where v is the electron beam velocity, ω_o is the TM_{110} mode frequency, ω_c is the cyclotron frequency ($eB/mc\gamma$), ε is the dimensionless coupling constant proportional to the e-beam current,[8] and Q is the cavity quality factor. The imaginary part of k is the growth rate; its reciprocal is the e-folding length of the unstable BBU mode.

This model also gives a timescale for maximum growth of the BBU excitation at a given distance, z :

$$t_{max} = \frac{z}{v_g} = \frac{z\left(\omega_c + 4\varepsilon Q^2 \omega_0\right)}{v\,\omega_c} \qquad (2)$$

where v_g is the group velocity of the BBU disturbance.

The measured RF power growth of 42 dB implies an RF amplitude growth of about 130 over 0.6 m, corresponding to an e-folding length of 12 cm. For the experimental parameters, eq. (1) gives an e-folding length of 27 cm, about a factor of two larger. This factor of two discrepancy may result from uncertainty in the following experimental parameters used in eq. (1): 1) Transported current was not equal to injected current, 2) Febetron voltage varied with time, 3) Experimental Q could be higher than the cold-test Q due to both the attachment of the intercavity copper tubes and the orthogonal polarization to the coupling, 4) Continuum theory may not be accurate for a 10 cavity system.

The e-folding length in the strong focusing regime is proportional to the inter-cavity spacing, so that the growth per cavity is expected to be independent of their spacing. This is in agreement with our observation that a change in spacing from 6 cm to 3 cm has little effect upon the BBU growth of the system.

The 10th cavity RF signal strength is plotted versus solenoidal magnetic field in Figure 4(a). The power in the BBU mode peaks at a magnetic field of about 2.5 kG. Figure 4(b) shows the ratio of transported current to magnetic field (I/B), plotted versus magnetic field. A peak at 2.5 kG is again observed. Equation (1) predicts that BBU growth is proportional to I/B, so that the coincidence of peaks at 2.5 kG in Figures 4(a) and 4(b) is consistent with theory.

The observed time to the onset of maximum RF power is presented in Figure 5, for comparison with theoretical values obtained with equation (2). The elapsed time from the beginning of the pulse to the RF peak in the tenth cavity is consistent with the theoretical values. It must be noted, however, that the Febetron voltage, and therefore v, ε, and ω_c, change over comparable time-scales, so that BBU growth may be impeded by the changing nature of the resonant growing mode. This, as well as the ability to access the "weak focusing regime," motivated the experiments on MELBA, described in the following section.

3.2 MELBA Experimental Results and Discussion

The MELBA BBU experiment utilized 5 cavities with spacing of 3 cm. RF power was measured in the second and fifth cavities. Data is shown in Figure 6 for two similar pulses. MELBA voltage is the uppermost trace followed by RF in the fifth cavity which has been attenuated by 20 dB, RF in the second cavity with no attenuation, transported current, and finally the lowermost trace is the injected current. The 2.5 GHz microwave power was found to increase by approximately 20 dB between the second and fifth cavities.

A plot of RF power versus magnetic field is given in Figure 7. On MELBA there was no correlation found between the level of 2.5 GHz microwave growth and the applied magnetic field. This is in fact consistent with theory which predicts that a "weak focusing" dispersion relation is independent of the magnetic field[3,7]. The "weak focusing" dispersion relation is:

$$k(\omega_0) = \frac{1}{v}\left\{\omega_0 \pm (1 + i)\omega_0\sqrt{\varepsilon Q}\right\} \tag{3}$$

Figure 8 shows the relationship between the RF power and e-beam current. The RF power was found to increase with increasing current as is expressed in the coupling factor, ε, of the dispersion relation.

From eq. (3), the BBU e-folding length is calculated to be 3 cm for the MELBA parameters. This implies 26 dB microwave power growth over the 9 cm separating the 2nd and 5th cavities, compared with 20 dB observed experimentally. Because 3 cm is not long compared with the cavity lengths and separation, the assumptions of continuum BBU theory are not rigorously satisfied[9]. Finite transit time effects are expected to reduce BBU growth compared with the prediction of the continuum theory. Nevertheless, the theory yields reasonable agreement with the observed behavior. Alternatively, matrix multiplication may be used to obtain more accurate predictions in this case.[10,11]

4. CONCLUSIONS

Initial experiments on the beam breakup instability have been performed on two long-pulse electron beam accelerators: MELBA and a Febetron. The following conclusions can be made:

1) The growth of TM_{110} radio frequency was found to increase at a rate of about 4.6 dB per cavity for the Febetron, which is twice the expected amount of BBU growth for those parameters.
2) The growth of TM_{110} radio frequency was found to increase at a rate of about 6.6 dB per cavity in the MELBA experiments, which is comparable to theory.
3) The Febetron BBU growth rates for the "strong focusing" regime show the expected dependence on the ratio of transported current to magnetic field.
4) The MELBA BBU growth rates for the "weak focusing" regime show the expected independence of magnetic field.
5) The growth rate in both the "strong" and "weak focusing" regimes shows the expected dependence on electron beam current.
6) The time required for the growth of the BBU disturbance is consistent with theory in the strong focusing regime.
7) In the strong focusing regime, BBU growth per cavity was nearly independent of cavity spacing, consistent with theory.

5. ACKNOWLEDGMENTS

This research was partially sponsored by SDIO-IST through an ONR contract. We would like to thank Dr. Y. Y. Lau for valuable consultations.

6. REFERENCES

1. W. K. H. Panofsky and M. Bander, "Asymptotic Theory of Beam Breakup in Linear Accelerators", Rev. Sci. Inst. 39, 206 (1968)
2. R. Helm and G. Loew, Beam Breakup, Chapter B.1.4 in *Linear Accelerators* (Eds. P.M. Lapostolle and A.L. Septier), North Holland Book Co. Amsterdam. 1970
3. Y. Y. Lau, "Asymptotic Growth of Cumulative and Regenerative Beam Breakup Instabilities in Accelerators", NRL Memo Report No. 6237 (1988)

4. P.R. Menge, R.A. Bosch, R.M. Gilgenbach, J.J. Choi, H. Ching, and T. Spencer, "Experiments on Long-pulse Electron Beam Transport Through Cavity Systems", Bulletin of the American Physical Society 35, 2070 (1990)
5. Y. Y. Lau, "Classification of Beam Breakup in Linear Accelerators", Phys. Rev. Lett. **63** 1141 (1989)
6. V.K. Neil, L.S. Hall, and R.K. Cooper, "Further Theoretical Studies of the Beam Breakup Instability", Part. Accel. **9**, 213 (1979)
7. R. A. Bosch and R. M. Gilgenbach, "Effect of X-Y Coupling on the Beam Breakup Instability", to appear in Appl. Phys. Lett., February 18, 1991
8. The formula for this ε factor is

$$\varepsilon = 0.422\frac{\ell}{L}\left(\frac{I}{17\text{kA}}\right)\frac{\beta}{\gamma}$$

where $\frac{\ell}{L}$ is the ratio of cavity length to intercavity distance, I is the e-beam current, and β and γ are the usual relativistic velocity and energy factors. A detailed explanation of this coupling constant can be found in reference 3.
9. D.G. Colombant and Y.Y. Lau, "Beam Breakup Instabilities in Linear Accelerators: Transition, Phase Mixing and Nonlinear Focusing", Appl. Phys. Lett. 53 2602 (1988)
10. D.G. Colombant, Y.Y. Lau, and D. Chernin, "Reduction of Beam Breakup Growth by Cavity Cross-Couplings in Recirculating Accelerators.", NRL Memorandum 6671, June 29, 1990.
11. Y.Y. Lau (private communication)

Table 1

Accelerator Comparison

	Febetron	MELBA
e-Beam Voltage	0.3 - 0.4 MV	0.6-1.0 MV
e-Beam Diode Current	0.1-1 kA	1-10 kA
e-Beam Current Extracted	20 - 100 A	100 - 400 A
e-Beam Pulselength	300 - 400 ns	0.5-5 μs
Beam Radius	0.5 cm	1.0 cm
Cavity Radius	6.9 cm	6.9 cm
Cavity TM_{110} mode frequency	2.5 GHz	2.5 GHz
Cavity TM_{010} mode frequency	1.6 GHz	1.6 GHz
Number of Cavities	10	5
Vacuum Chamber Radius	7.4 cm	7.4 cm
Cavity System Length	0.6 m	0.2 m

Table 2

Cavity Parameters

	TM_{110} Mode Frequency (GHz)	TM_{110} Q
Cavity # 1	2.509	190
Cavity # 2	2.510	210
Cavity # 3	2.510	220
Cavity # 4	2.515	200
Cavity # 5	2.507	240
Cavity # 6	2.510	190
Cavity # 7	2.510	210
Cavity # 8	2.508	160
Cavity # 9	2.515	210
Cavity # 10	2.510	220

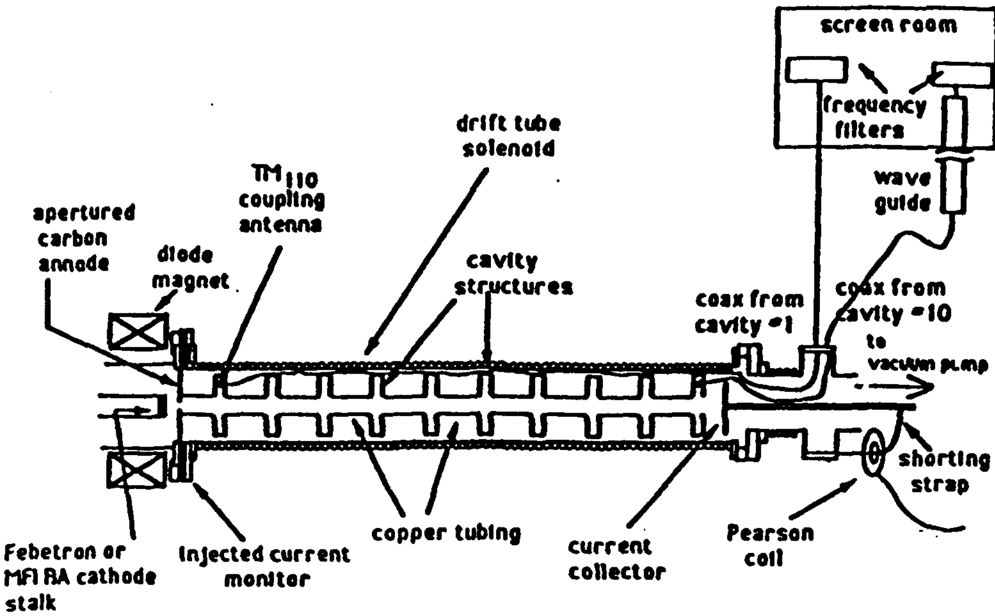

Figure 1. Experimental Configuration

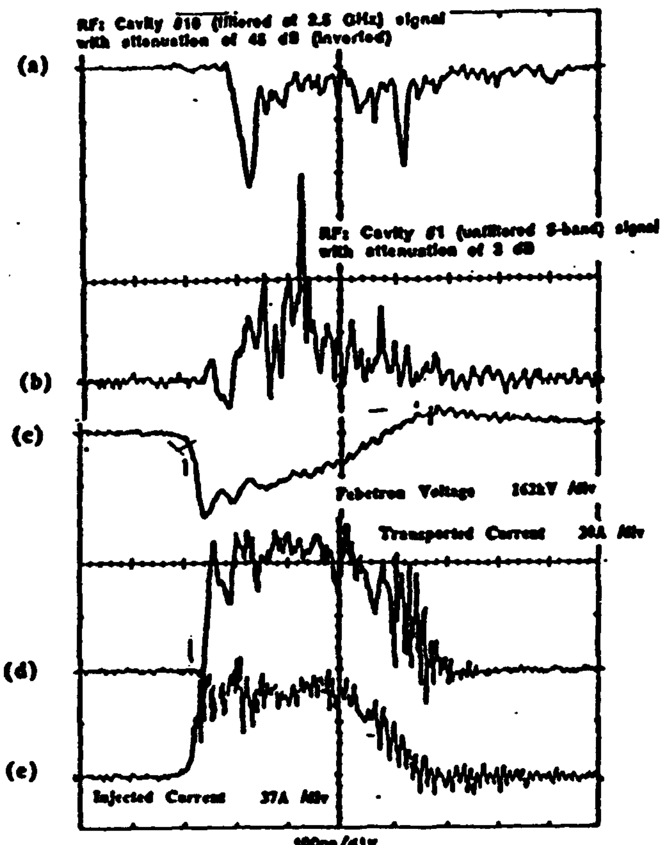

Figure 2. Data taken in two Febetron shots at a magnetic field of 2.52 kG a) 10th cavity 2.5 GHz RF signal attenuated by 45 dB (200 mV/div), b) 1st cavity full S-band (100mV/div) RF signal attenuated by 3 dB, c) Diode voltage pulse (162 kV/div), d) Transported current (20 A/div), e) Injected current (37 A/div)

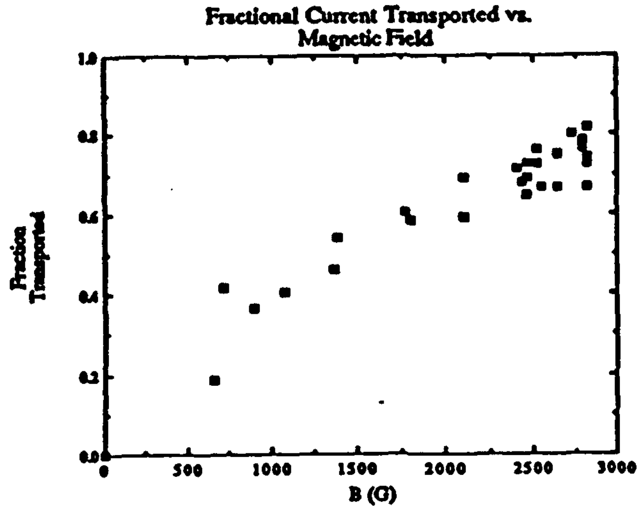

Figure 3. Fraction of current transported versus magnetic field for Febetron

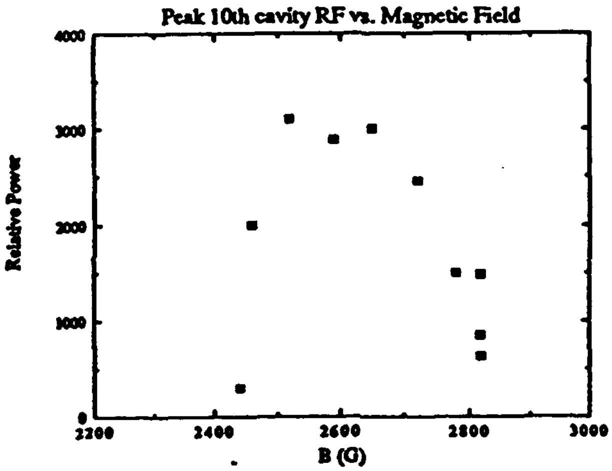

Figure 4a. Peak 10th cavity RF (2.5 GHz) signal vs. magnetic field for Febetron

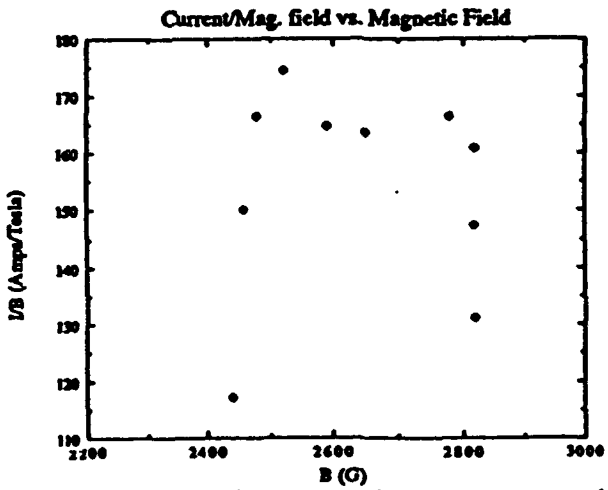

Figure 4b. Ratio of transported current to magnetic field vs. magnetic field for Febetron

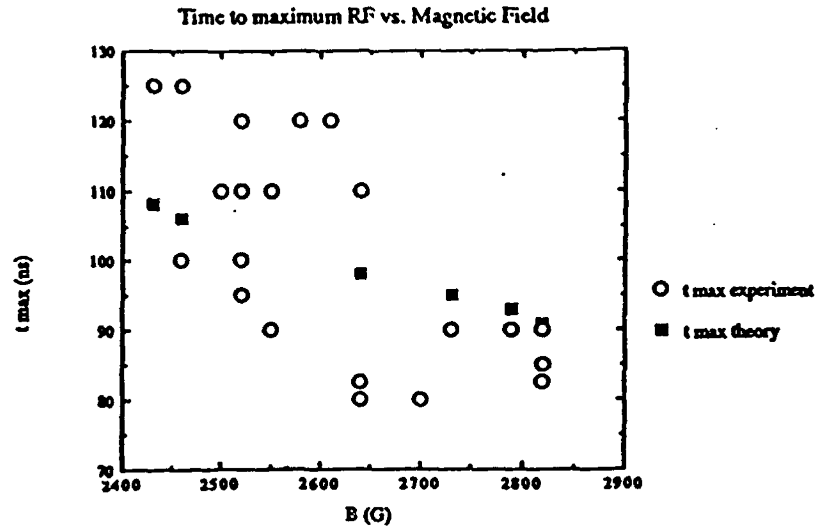

Figure 5. Comparison of experimental time to RF peaking (2.5 GHz) to the theoretical value of time to maximum BBU growth rate

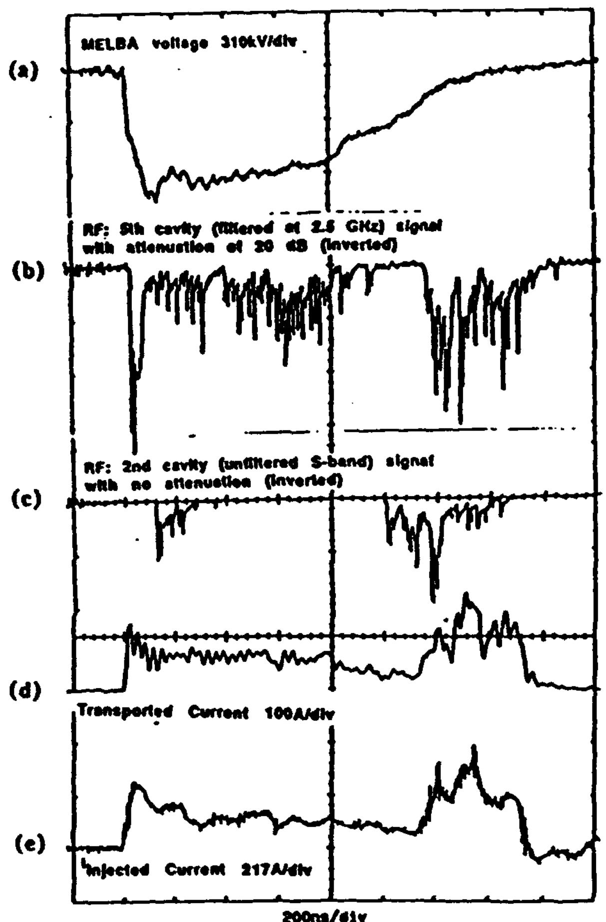

Figure 6. Data from two similar MELBA shots at a magnetic field of 2.95 kG a) MELBA diode voltage pulse (310 kV/div), b) 5th cavity 2.5 GHz RF signal attenuated by 20 dB (20 mV/div), c) 2nd cavity full S-band signal (no attenuation) (50 mV/div), d) Transported current (100A/div), e) Injected cu rent (217 A/div)

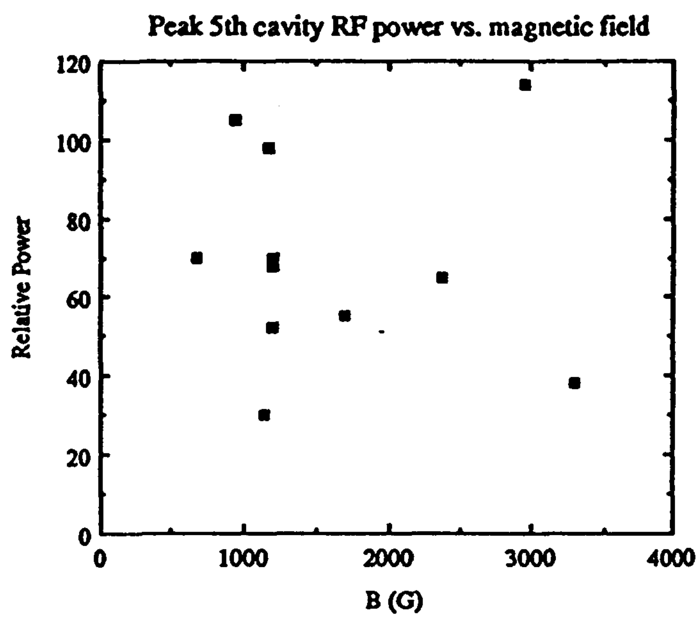

Figure 7. Peak RF power in the 5th cavity versus applied magnetic field for MELBA

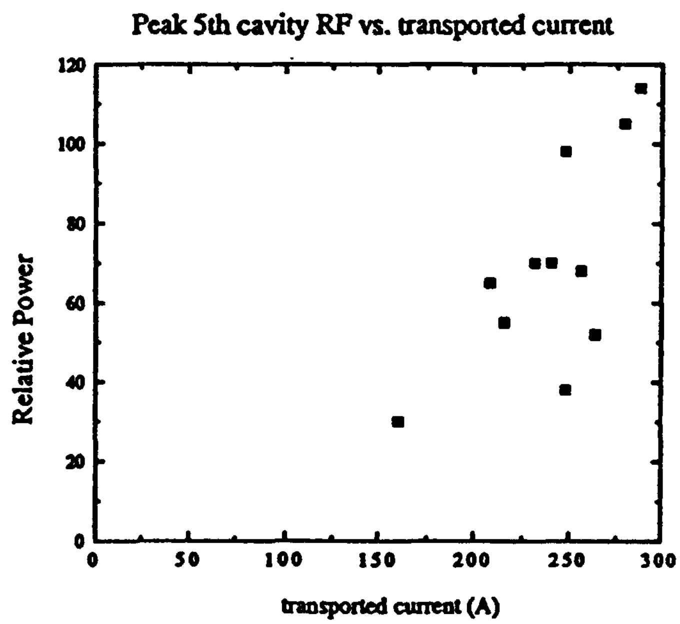

Figure 8. Peak RF power in the fifth cavity versus the transported current for MELBA